NONLINEAR NUMERICAL FLIGHT DYNAMICS FOR THE PREDICTION OF MANEUVER LOADS

Markus Ritter[1] **and Johannes Dillinger**[1]

[1]DLR - Institute of Aeroelasticity
Bunsenstraße 10, 37073 Göttingen
Markus.Ritter@dlr.de
Johannes.Dillinger@dlr.de

Keywords: Numerical Flight Dynamics, Fluid-Structure-Interaction, CFD, FE, CSM, TAU, Maneuver Loads, 6-DOF, Elastic Aircraft

Abstract: Dynamic analysis of flexible aircraft typically involves the separation of rigid body and structural dynamics. This approach is justified, if an adequate distance between the frequencies of the elastic and the flight mechanic modes is present. For aircraft structures characterized by relatively low elastic frequencies (e.g. large passenger aircraft or sailplanes) the combined calculation of the coupled rigid body and structural dynamics becomes important and the setup of an integrated aeroelastic model of the aircraft is necessary.
This article describes the derivation of the integrated aeroelastic model, composed of governing equations for the translational, the rotational, and the elastic motion. A modal approach is used for the calculation of the elastic deformations of the aircraft, therefore using unconstrained free-free vibration modes from a Finite-Element analysis. The aerodynamic forces are calculated by a CFD solver in Arbitrary Lagrangian Eulerian (ALE) formulation. The integration of all involved disciplines is finally done via a weak coupling approach applying a CSS (Conventional-Serial-Staggered) algorithm. The integrated model is intended to be used for the prediction of maneuver or gust loads.

1 INTRODUCTION

This article presents a method for the numerical simulation of flight dynamics of an aircraft in the time domain where elastic deformations of the structure receive particular attention.
Most approaches treating dynamic analysis of flexible aircraft assume a comparatively high ratio of elastic structural frequencies and rigid body eigenfrequencies. Therefore, the involved disciplines describing the elastic deformations on the one hand and the translational and rotational displacements of the structure on the other hand, can be analysed independently of each other due to low mutual interaction. As the frequency ratio decreases notably, elastic structural and flight mechanic modes interact by reason of aerodynamic and inertia forces since low-frequency structural eigenmodes imply a flexible aircraft structure leading to larger elastic deformations during flight maneuvers.
A further and often applied simplification in the description of aicraft flight dynamics is the use of linearized aerodynamic models comprising the potential theory in many cases. These models are certainly restricted in terms of nonlinear aerodynamic effects arising at transonic Mach numbers and in viscous flows. The method presented here includes aerodynamic forces obtained from an unsteady CFD simulation. Thus fewer restrictions concerning the flow characteristics are made and both inviscid Euler and viscous Navier-Stokes models capturing relevant aerodynamic nonlinearities like shocks or flow separations can be applied. The application of aerodynamic models of different fidelity enables

the simulation of flight maneuvers in the entire flight envelop of the aircraft.
The derivation of governing equations for the integrated aeroelastic model is described in the first chapter, while the second one presents simulation results obtained with this model applied on a generic test aircraft. The derived model adresses applications for the simulation of e.g. prescribed flight maneuvers and gust encounters, as well as fight mechanic stability analysis, to name a few.

2 THE DERIVATION OF THE INTEGRATED AEROELASTIC MODEL

In the first section, the derivation of the integrated aeroelastic model including the rigid body and elastic degrees of freedom governing equations as well as the methods for the spatial and temporal integration of the CFD aerodynamic model are described.

2.1 Governing equations of translational and rotational motion (6-DOF motion) of a body

The governing equations describing the dynamic of the elastic aircraft have been addressed by many authors (e.g. Waszak and Schmidt [1] or Waszak and Buttril [2]). The starting point is the description of an elastic body as a continuous distribution of mass elements. The position of the mass elements is described in a noninertial, local body-reference coordinate system which in turn is described relative to an inertial geodetic (earth-fixed) reference frame (cf. Fig. 1).

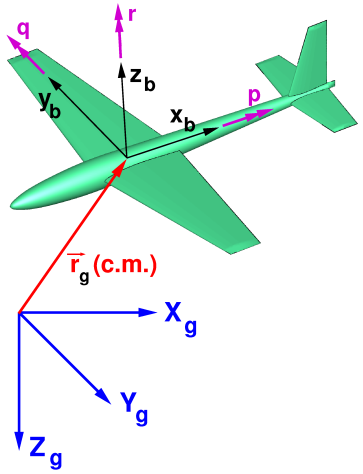

Figure 1: Two different coordinate systems for the description of motions of the aircraft: geodetic (inertial) reference frame, index g, and body fixed frame, index b. The angular velocity of the aircraft in the body fixed frame is denoted by p, q, and r.

To avoid *inertial coupling* between the rigid- and the elastic degrees of freedom, a proper choice has to be made for the position and the orientation of the body reference coordinate system. The use of *mean axis* minimizes the degree of inertial coupling [1]. A mean axis reference frame is positioned such that its origin always coincides with the instantaneous center of gravity of the body.
The calculation of the translational motion of the aircraft follows Newton's law expressed in the geodetic reference frame. The resulting forces $\mathbf{F}^g$ acting on the center of gravity of the aircraft are composed of the aerodynamic forces $\mathbf{F}^b_a$, the external applied forces $\mathbf{F}^g_{ext}$ (e.g. thrust), and the gravity forces $\mathbf{F}^g_g$. Since the aerodynamic forces are in that case

obtained from a CFD solver, which outputs them in the body-fixed reference frame, they have to be rotated into the geodetic frame using a rotation matrix $\mathbf{A}^{gb}$. In terms of the geodetic reference frame, the translational governing equations become

$$\mathbf{F}^g = \mathbf{A}^{gb}\,\mathbf{F}_a^b + \mathbf{F}_{ext}^g + \mathbf{F}_g^g = m \cdot \ddot{\mathbf{r}}_{c.m.}^g \tag{1}$$

where m denotes the mass of the aircraft, which can be simply obtained by summing up the entries of the lumped mass matrix of the corresponding Finite-Element model of the aircraft. The vector $\mathbf{r}_{c.m.}^g$ describes the position of the center of mass of the aircraft (or the origin of the body fixed frame, respectively) with respect to the geodetic frame.

The rotational motion of the aircraft is governed by Euler's dynamic equations of motion. Depending on the orientation of the axis of the body-fixed reference frame, they can either be formulated for the principal axis of inertia and are consequently written as:

$$\begin{aligned} M_1^b &= I_1\dot{\omega}_1^b - (I_2 - I_3)\omega_2^b\omega_3^b \\ M_2^b &= I_2\dot{\omega}_2^b - (I_3 - I_1)\omega_3^b\omega_1^b \\ M_3^b &= I_3\dot{\omega}_3^b - (I_1 - I_2)\omega_1^b\omega_2^b \end{aligned} \tag{2}$$

with M_i^b denoting the moments acting on the aircraft around the body axis, composed of aerodynamic and external moments. For any orientation of the body axis defined by convenience (denoted by ϕ, θ, and ψ), the general form becomes

$$\begin{aligned} I_{xx}\,\dot{p} - (I_{xy}\,\dot{q} + I_{xz}\,\dot{r}) + (I_{zz} - I_{yy})q\,r + (I_{xy}r - I_{xz}q)p + (r^2 - q^2)\,I_{yz} &= M_\phi^b \\ I_{yy}\,\dot{q} - (I_{xy}\,\dot{p} + I_{yz}\,\dot{r}) + (I_{xx} - I_{zz})p\,r + (I_{yz}p - I_{xy}r)q + (p^2 - r^2)\,I_{xz} &= M_\theta^b \\ I_{zz}\,\dot{r} - (I_{xz}\,\dot{p} + I_{yz}\,\dot{q}) + (I_{yy} - I_{xx})p\,q + (I_{xz}q - I_{yz}p)r + (q^2 - p^2)\,I_{xy} &= M_\psi^b \end{aligned} \tag{3}$$

where I_{ii} denotes a moment of inertia, and p, q, r the angular rates about the body axis x_b, y_b, and z_b, respectively. In Eqns. 2 and 3 the inertia tensor I of the aircraft is assumed to be constant. To obtain the angular orientation of the body fixed frame with respect to the inertial frame, a temporal integration of the angular velocity calculated from Eqn. 2 or 3, respectively, is necessary. A convenient method for the mathematical description of spatial orientations and rotations is given by quaternions, an extension of the complex numbers. The advantage over the Euler angles usually used in aircraft dynamics is the avoidance of singularities at certain rotation angles (gimble lock). The following differential equation describes the relation between the angular rates p, q, and r and the quaternion parameters q_0, q_1, q_2, and q_3 [3]:

$$\begin{pmatrix} \dot{q}_0 \\ \dot{q}_1 \\ \dot{q}_2 \\ \dot{q}_3 \end{pmatrix} = \frac{1}{2} \begin{pmatrix} 0 & -p & -q & -r \\ p & 0 & r & -q \\ q & -r & 0 & p \\ r & q & -p & 0 \end{pmatrix} \begin{pmatrix} q_0 \\ q_1 \\ q_2 \\ q_3 \end{pmatrix} \tag{4}$$

The rotation matrix A^{gb} can be calculated using the quaternion parameters obtained from Eqn. 4 [3] with

$$\mathbf{A}^{gb} = \begin{pmatrix} q_0^2 + q_1^2 - q_2^2 - q_3^2 & 2\,(q_1\,q_2 + q_0\,q_3) & 2\,(q_1\,q_3 - q_0\,q_2) \\ 2\,(q_1\,q_2 - q_0\,q_3) & q_0^2 - q_1^2 + q_2^2 - q_3^2 & 2\,(q_2\,q_3 + q_0\,q_1) \\ 2\,(q_1\,q_3 + q_0\,q_2) & 2\,(q_2\,q_3 - q_0\,q_1) & q_0^2 - q_1^2 - q_2^2 + q_3^2 \end{pmatrix} \tag{5}$$

Equations 1, 2 or 3, and 4 completely describe the 6-DOF motion of the aircraft in terms of the geodetic coordinate system and can be written combined and in short as

$$\frac{d\,\mathbf{U}}{d\,t} + \mathbf{R}^{AC}\,(t,\ \mathbf{U}) = 0 \tag{6}$$

with $\mathbf{U}$ as the vector of unknowns:

$$\mathbf{U} = \left[\begin{pmatrix} r^{\,g}_{c.m.,\,x} \\ r^{\,g}_{c.m.,\,y} \\ r^{\,g}_{c.m.,\,z} \end{pmatrix}^T, \begin{pmatrix} \dot{r}^{\,g}_{c.m.,\,x} \\ \dot{r}^{\,g}_{c.m.,\,y} \\ \dot{r}^{\,g}_{c.m.,\,z} \end{pmatrix}^T, \begin{pmatrix} p \\ q \\ r \end{pmatrix}^T, \begin{pmatrix} q_0 \\ q_1 \\ q_2 \\ q_3 \end{pmatrix}^T \right]^T \tag{7}$$

Equation 6 is a system of nonlinear, inhomogeneous, first order differential equations in time. It is not stiff and can be solved by any standard numerical scheme suitable for this type of equation. In this case, Heun's method was applied, a semi-implicit predictor-corrector scheme that provides second-order temporal accuracy. Using this method, the corrector step of Eqn. 6 becomes in discretised form (with h as the time step size):

$$\mathbf{U}_{i+1} = \mathbf{U}_i + \frac{h}{2}\left(\mathbf{R}^{AC}(t_i, \mathbf{U}_i) + \mathbf{R}^{AC}\Big(t_{i+1}, \mathbf{U}_i + h\,\mathbf{R}^{AC}(t_i, \mathbf{U}_i)\Big)\right) \tag{8}$$

The term

$$\mathbf{U}_i + h\,\mathbf{R}^{AC}(t_i, \mathbf{U}_i)$$

denotes the result of the predictor step (equivalent to a *forward Euler* step).

2.2 Governing equations of the structural deformation

As described in Section 2.1, the use of a mean axis reference frame avoids an inertial coupling between structural deformations and rigid body degrees of freedom. The mean axis constraint can be fulfilled by using elastic mode shapes calculated from an *unconstrained* (free-free) structural model [2]. The equation of motion for the forced vibration problem in generalised coordinates with modal (Rayleigh) damping is given as:

$$\ddot{\mathbf{q}}^{\,b}(t) + 2\,\xi\,\omega\,\dot{\mathbf{q}}^{\,b}(t) + \omega^2\,\mathbf{q}^{\,b}(t) = \tilde{\phi}_S^T\,\mathbf{F}^{\,b}(t) \tag{9}$$

Vector $\mathbf{q}(t)$ is composed of the generalised displacements, ξ denotes the damping matrix (composed of linear combinations of the stiffness and mass values for the respective mode shape), and ω^2 contains the structural eigenvalues. The right-hand side consists of the generalised forces as the product of the transposed matrix of the (mass normalised) eigenvectors, $\tilde{\phi}_S^T$, and the forces $\mathbf{F}^{\,b}(t)$. When applied to calculate the structural dynamics of a moving aircraft, the force vector $\mathbf{F}^{\,b}(t)$ includes inertia forces due to translational and rotational motion of the aircraft:

$$\mathbf{F}^{\,b}(t) = \mathbf{F}^{\,b}_{aero,\,S}(t) - \mathbf{M}\cdot\left(\mathbf{A}^{gb^T}\mathbf{g} + \ddot{\mathbf{r}}^{\,g}_{c.m.} + \dot{\omega}^b \times \mathbf{r}_{0'P} + \omega^b \times (\omega^b \times \mathbf{r}_{0'P})\right) \tag{10}$$

$\mathbf{M}$ denotes the (lumped) mass matrix of the structure, ω^b consists of the angular velocities p, q, r, $\mathbf{g}$ is the gravity vector, and $\mathbf{r}_{0'P}$ describes the position of each discrete mass point of the mass matrix in terms of the body-fixed reference frame for the undeformed structure. To transform the forces $\mathbf{F}^{\,b}_{aero}(t)$ obtained from the CFD solver at the CFD mesh points to equivalent forces acting on the structural nodes, the transposed of an interpolation

matrix $\mathbf{H}$, build of radial basis functions, is used. The structural displacements u^b, on the other hand, are interpolated onto the CFD mesh using the same interpolation matrix $\mathbf{H}$ [4]:

$$\mathbf{F}^{\,b}_{aero,\,S}(t) = \mathbf{H}^T\ \mathbf{F}^{\,b}_{aero}(t), \quad \mathbf{u}^{\,b}_{aero}(t) = \mathbf{H}\ \mathbf{u}^{\,b}_{S}(t) \tag{11}$$

This approach ensures a (global) conservative force transformation [4]. A scheme particularly suited for the solution of Eqn. 9 is the Newmark-beta method due to its low numerical dissipation. It can be written as a predictor-corrector scheme (superscripts p and c) and becomes [4]:

$$\begin{aligned}
\mathbf{q}^{\,p}_{i+1} &= \mathbf{B}_1^{-1}\,\mathbf{F}^{\,b}_{i} + \left(\mathbf{B}_1^{-1}\,\mathbf{B}_2\right)\mathbf{q}_i + \left(\mathbf{B}_1^{-1}\,\mathbf{B}_3\right)\dot{\mathbf{q}}_i + \left(\mathbf{B}_1^{-1}\,\mathbf{B}_4\right)\ddot{\mathbf{q}}_i \\
\mathbf{q}^{\,c}_{i+1} &= \mathbf{B}_1^{-1}\,\mathbf{F}^{\,b}_{i+1} + \left(\mathbf{B}_1^{-1}\,\mathbf{B}_2\right)\mathbf{q}_i + \left(\mathbf{B}_1^{-1}\,\mathbf{B}_3\right)\dot{\mathbf{q}}_i + \left(\mathbf{B}_1^{-1}\,\mathbf{B}_4\right)\ddot{\mathbf{q}}_i
\end{aligned} \tag{12}$$

with

$$\mathbf{B}_1 = \mathbf{I}\,\frac{1}{\gamma\,h^2} + \xi\,\frac{\delta}{\gamma\,h} + \omega^2, \quad \mathbf{B}_2 = \mathbf{I}\,\frac{1}{\gamma\,h^2} + \xi\,\frac{\delta}{\gamma\,h}$$

$$\mathbf{B}_3 = \mathbf{I}\,\frac{1}{\gamma\,h} + \xi\left(\frac{\delta}{\gamma} - 1\right), \quad \mathbf{B}_4 = \mathbf{I}\left(\frac{1}{2\,\gamma} - 1\right) + \xi\,h\left(\frac{\delta}{2\,\gamma} - 1\right)$$

where $\mathbf{I}$ denotes the identitiy matrix and the constants γ and δ are given the values 0.5 and 0.25, respectively, which ensures that the scheme is implicitly stable.

2.3 Temporal coupling of 6-DOF motion and structural deformations

The remaining task is the temporal coupling of the 6-DOF motion, the structural deformations, and the CFD computations. Therefore, a modified Conventional Serial Staggered (CSS) algorithm is applied. In the predictor step, the aerodynamic forces from the CFD simulation are transformed to equivalent structural forces via Eqn. 11. Using these forces, the vector of unknowns $\mathbf{U}$ (cf. Equation 7) is calculated by solving Eqn. 6, and the structural deformations are calculated solving Eqn. 12. The predicted translational and rotational movements and the structural deformations are used to update the kinematic boundary conditions in the flow solver. Subsequently, new aerodynamic forces are calculated and the steps described above are repeated in the corrector step. The described CSS algorithm is sketched in Figure 2.

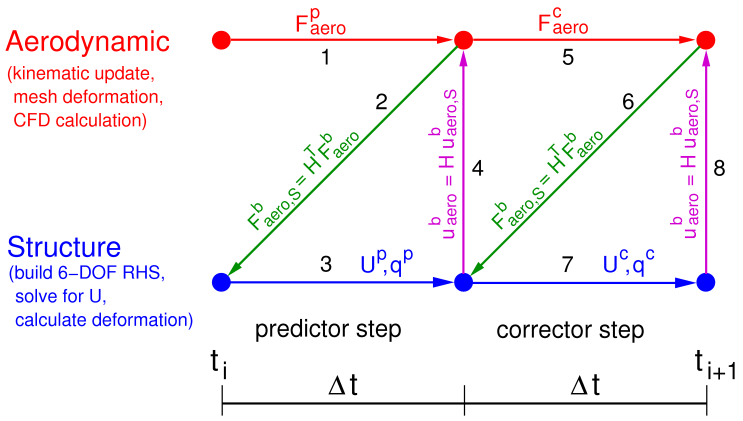

Figure 2: Illustration of the temporal coupling approach between the aerodynamic and the structural calculations.

2.4 Validation of the flight dynamic module

The implemented Heun method for the temporal integration was validated against some analytical test cases describing motions of mass points. The results for an oscillator without damping and for a falling sphere subjected to aerodynamic drag are shown in Fig. 3 and 4. Both plots show the full match of numerical and anylytical results. The implemented CSS algorithm in combination with the described interpolation method for forces and deformations has been validated against several test cases, see [5] for instance.

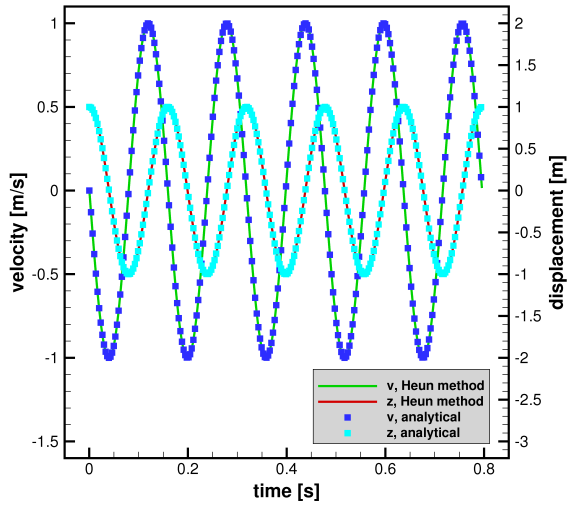

Figure 3: Validation of the implemented Heun method against the analytical solution of an harmonic oscillator:
$\ddot{x}(t) + \omega^2 x(t) = 0.$
Parameters: $\omega = \sqrt{\frac{k}{m}} = 1.0.$
$x(t=0) = \dot{x}(t=0) = 1.0.$

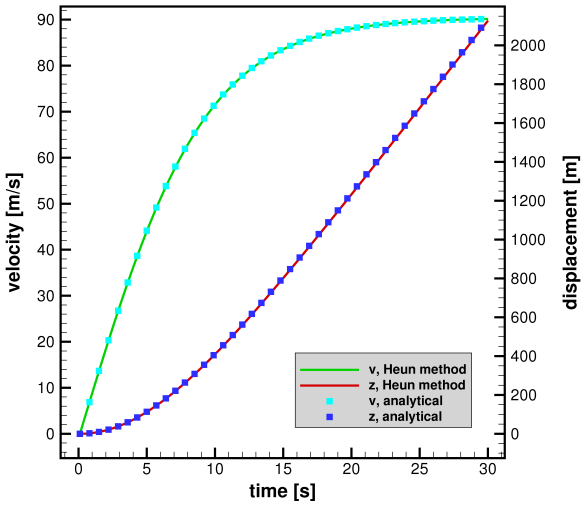

Figure 4: Validation of the implemented Heun method against the analytical solution of a falling sphere with aerodynamic drag:
$g - \ddot{x}(t) - \alpha \dot{x}^2(t) = 0.$
Parameters: $\alpha = \frac{\rho c_D A_{ref}}{2m} = 0.0012/m.$

3 FLIGHT SIMULATIONS WITH A GENERIC AIRCRAFT CONFIGURATION

This section presents results of simple flight maneuvers using the approach described in Section 2. The aircraft used has a generic configuration, the discretised model consists of a relatively coarse Euler CFD mesh and a Finite-Element model made of *CQUAD4* shell elements. Any CFD calculations are performed with the DLR TAU-code, a Finite-Volume flow solver in Arbitrary Lagrangian Eulerian (ALE) formulation, capable of handling mesh deformations and prescribed kinematic boundary conditions on moving surfaces [6]. The CFD mesh of the generic aircraft and the Finite-Element model together with the first bending mode shape are shown in Fig. 5 and Fig. 6.

3.1 Trimming approach for the steady horizontal flight

As a starting point for the simulation of dynamic maneuvers, the aircraft needs to be in a steady horizontal flight state, requiring that the sum of all forces (drag forces are

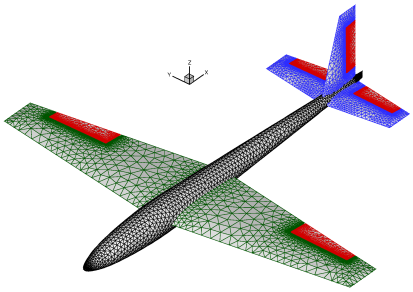

Figure 5: CFD mesh of the generic aircraft used for flight dynamic analysis.

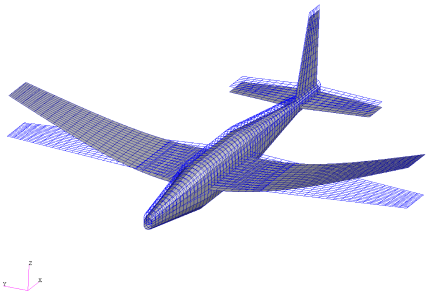

Figure 6: Finite-Element model of the generic aircraft and first bending mode shape of the unconstrained, free-free model.

cancelled by thrust) as well as all moments acting on the center of gravity become zero (in the case that no external moments due tue e.g. thrust are present). Newton's method is applied iteratively to this problem in order to calculate the pitch angle θ and the elevator deflection η of the aircraft:

$$\begin{pmatrix} \theta \\ \eta \end{pmatrix}_{i+1} = \begin{pmatrix} \frac{\partial C_A}{\partial \theta} & \frac{\partial C_A}{\partial \eta} \\ \frac{\partial M_y}{\partial \theta} & \frac{\partial M_y}{\partial \eta} \end{pmatrix}_i^{-1} \cdot \begin{pmatrix} \tilde{C}_A - C_A(\theta_i, \eta_i) \\ -M_y(\theta_i, \eta_i) \end{pmatrix}_i + \begin{pmatrix} \theta \\ \eta \end{pmatrix}_i \tag{13}$$

The resulting structural deformation for the steady horizontal flight state of the aircraft is shown in Fig. 7. The contribution of the different mode shapes of the aircraft structure is depicted in Fig. 8. The deformation at the steady horizontal flight is significantly dominated by the first bending mode shape.

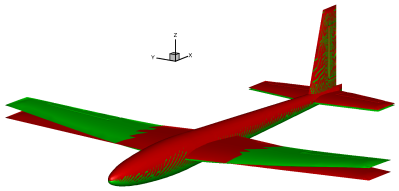

Figure 7: Undeformed aircraft structure and deformation at steady horizontal flight.

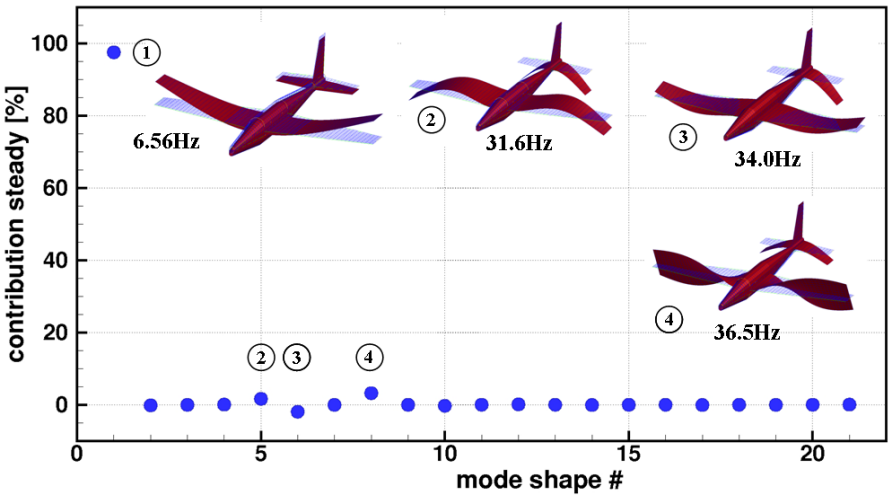

Figure 8: Contribution of the different structural mode shapes to the entire elastic deformation of the aircraft in steady horizontal flight.

3.2 Simulation results of simple dynamic maneuvers

The results of two simple dynamic flight simulations are presented. Structural deformations are illustrated in terms of the first bending mode since the contribution of this mode shape to the entire deformation is more than 95%. First, a pull up manoeuver with three different elevator deflections, depicted in Fig. 9 and 10. To display the effects of the structural elasticity, the simulation was performed with a stiff aircraft, additionally. The center of pressure is located ahead of the elastic axis, resulting in an increased torsional moment when the AoA is increased and therefore in an increased lift. Second, a menoeuver where the elevator is deflected in the resonance frequency of the first bending mode, shown in Fig. 11 and 12. The coupling between the structural and the flight mechanic degrees of freedom becomes evident after the excitation is stopped, the ongoing (and only slightly damped) oscillation of the wing causes the C.G. to move as well.

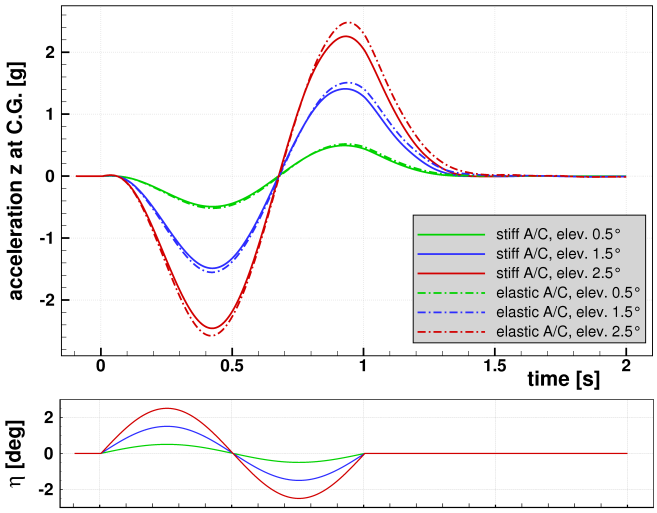

Figure 9: Response of the acceleration in z-direction at the center of gravity (C.G.) for sinusoidal elevator input with different amplitudes.

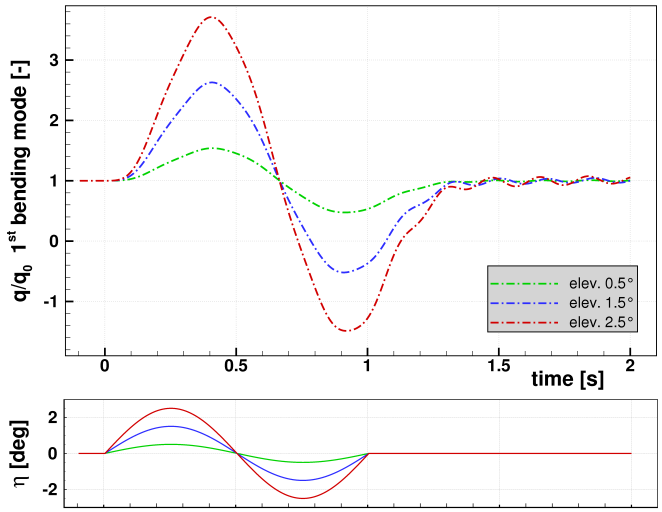

Figure 10: Response of the normalised generalised displacement of the first bending mode for sinusoidal elevator input with different amplitudes.

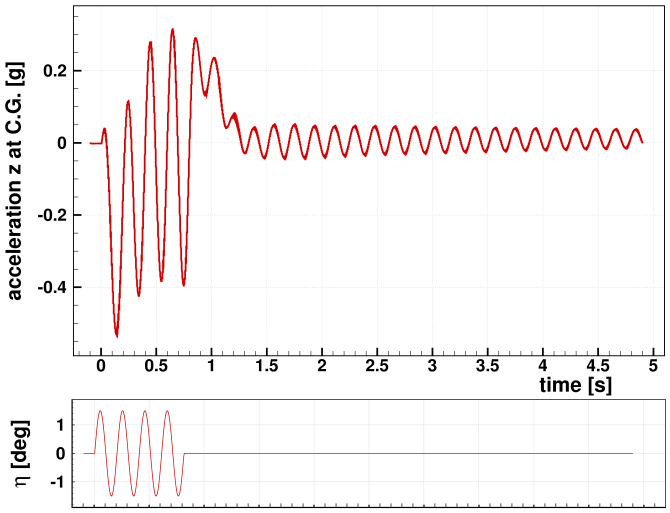

Figure 11: Response of the acceleration in z-direction at the center of gravity (C.G.) for elevator deflection with the frequency of the first bending mode shape.

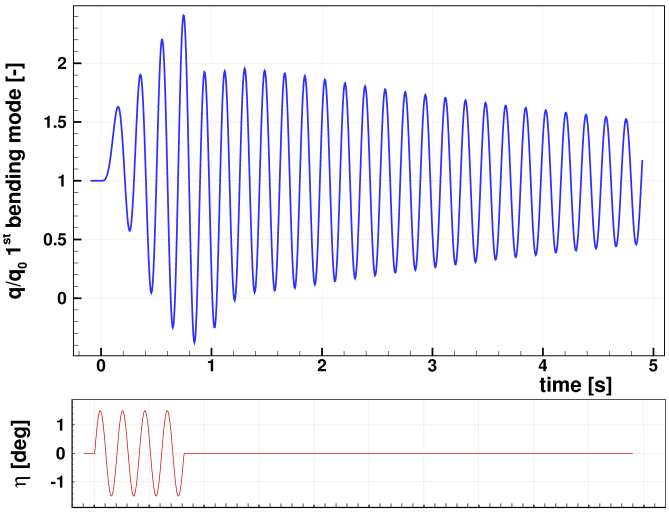

Figure 12: Response of the normalised generalised displacement of the first bending mode for elevator deflection with the frequency of the first bending mode.

4 CONCLUSION

Though only a few simulation results of the presented method have been shown, it could be demonstrated that this approach should be able to serve as a simulation environment for the determination of aerodynamic and structural loads due to prescribed maneuvers as well as loads due to gust encounter. The advantage of the use of CFD methods is that the fidelity can be chosen (e.g. Euler and Navier-Stokes models) and aerodynamic nonlinearities are captured. Nevertheless, the computational effort of this method is higher compared to the use of aerodynamic models based on potential theory. The method will be enhanced with terms describing structural nonlinearities (both in the equations describing the rotational dynamics and the elastic deformations of the aircraft) that enable the simulation of maneuvers with high, nonlinear elastic deformations.

5 REFERENCES

[1] Waszak, M. and Schmidt, D. (1988). Flight dynamics of aeroelastic vehicles. Tech. Rep. Vol. 25, No.6, Journal of Aircraft.

[2] Waszak, M., Buttrill, C., and Schmidt, D. (1992). Modeling and model simplification of aeroelastic vehicles: An overview. Tech. rep., NASA Langley Research Center. NASA-TM-107691.

[3] Stevens, B. L. and Lewis, F. L. (1992). *AIRCRAFT CONTROL AND SIMULATION*. JOHN WILEY & SONS, INC. ISBN 0-471-61397-5.

[4] Beckert, A. and Wendland, H. (2001). Multivariate interpolation for fluid-structure-interaction problems using radial basis functions. Tech. Rep. 5152, Aerospace Science and Technology.

[5] Neumann, J. and Ritter, M. (2009). Steady and unsteady aeroelastic simulations of the hirenasd wind tunnel experiment. Proceedings, IFASD 2009 ,Seattle.

[6] DLR. *Homepage of DLR TAU code*. URL: http://tau.dlr.de.